Statistical Analysis of GSNR Fluctuations Due to Physical Layer Uncertainties

Giacomo Borraccini*, Andrea D'Amico, Andrea Carena, and Vittorio Curri
Department of Electronics and Telecommunications - Politecnico di Torino, Turin, Italy
*giacomo.borraccini@polito.it

***Abstract*—We present an analytical model based on the uncertainty propagation theory for the generalized signal-to-noise ratio (GSNR) error estimation at the output of an optical line system due to connector loss and amplifier gain ripple uncertainties. The results are validated by comparison with a Monte Carlo analysis, showing an excellent agreement in terms of estimated GSNR average and standard deviation.**

***Index Terms*—Optical fiber communications, uncertainty modelling, nonlinear interference, amplified spontaneous emission.**

I. Introduction

The continuous growth in the demand for data traffic directly impacts the need for larger capacity in optical networks, starting from the back-bone segment [1]. To sustain this request, operators aim to fully exploit the installed infrastructures in order to maximize returns on investments. A simple but effective approach is to increase the capacity of installed equipment by minimizing system margins in lightpath deployment [2]. Margins are usually adopted to avoid out-of-service due to aging, soft-failures and working point variations related to network elements.

We focus on fluctuations of the working point at the transmission layer and specifically on the role of the power control in optical line systems (OLS)s. It is well accepted that the unique meter for quality-of-transmission (QoT) in optical networks is the generalized signal-to-noise ratio, GSNR, [3], [4] that includes both the effects of the amplified spontaneous emission (ASE) noise, P_{ASE}, due to in-line amplifiers (ILA)s and of the nonlinear interference, P_{NLI}, generated by fiber propagation. The GSNR is expressed as follows:

$$\mathrm{GSNR} = \frac{P_{ch}}{P_{\mathrm{ASE}} + P_{\mathrm{NLI}}} = \left(\mathrm{OSNR}^{-1} + {\mathrm{SNR}_{\mathrm{NL}}}^{-1}\right)^{-1} \quad (1)$$

where P_{ch} is the channel signal power, $\mathrm{OSNR} = P_{ch}/P_{\mathrm{ASE}}$ and $\mathrm{SNR}_{\mathrm{NL}} = P_{ch}/P_{\mathrm{NLI}}$. The GSNR presents a maximum at the optimal power that induces the best trade-off between the impairments of the ASE and NLI noises [5]. Operating at the optimal working point implies a larger attainable GSNR than working in the linear regime. Furthermore, the relevant benefit of this choice is also to reduce the effect of optical component uncertainties.

In this work, we extend the analyses of [6] to show how operating at the optimal nonlinear propagation regime mitigates the variations on the GSNR caused by the two main sources of uncertainty in an OLS: the *connector loss* defining the actual input power of the fiber span and the *gain ripple* of ILAs. We present a simple analytical model based on the uncertainty propagation which enables the estimation of the GSNR error at the OLS output given the connector loss and gain ripple error distributions. The results are verified by a comparison with a Monte Carlo analysis that emulates the impairment due to components' uncertainty in channel propagation through the OLS, showing an evident matching with the proposed model.

II. Scenario and Analytical Model

As depicted in Fig. 1, we consider a periodic OLS composed of 20 fiber spans, each characterized by a connector, an 80 km long standard single mode fiber (SSMF) and an erbium-doped fiber amplifier (EDFA). At the OLS input, we transmit 91 PM-MQAM coherent channels, which are assumed to be transmitted with a 50 GHz fixed WDM grid in the C-band (191.45-195.95 THz). Each channel has a root raised cosine spectral shape with a symbol rate, B_r, of 32 GBaud. The connector loss average is 0.75 dB and the fiber has a loss coefficient of 0.19 dB/km, dispersion coefficient of 16.7 ps/nm/km and an effective area of 80 μm^2. EDFAs operate in transparency mode, recovering the previous fiber span total loss, A, and restoring the signal power to the injected level at the beginning of the span. Each amplifier presents a flat noise figure, NF, of 5.3 dB and a frequency-dependent gain ripple profile. The NLI estimation is obtained through the GN-model [7]. We do not consider inter-channel Raman scattering in this study as the proposed approach focuses on the central channel of the spectrum, but the model can be further generalized including this effect.

In the analyzed scenario, we consider the presence of two sources of uncertainty: the connector loss at the fiber span input and the gain ripple profile of the EDFA. Assuming symmetrical input probability distribution functions (PDF)s of connector losses and gain ripples, we derive a simple analytical model based on uncertainty propagation to estimate the GSNR error due to connector and ILA impairments at the output of the periodic OLS. Firstly, we derive the expression of the GSNR_i at the output of the periodic OLS considering each input connector loss, l_n, and amplifier gain ripple profile, $g_{n,i}$, as a random variable; the indices n and i refer to a certain fiber span within the OLS and to a specific channel of the spectrum, respectively. As a consequence, we describe each random variable associating a PDF with defined values of average and standard deviation, σ_{l_n}, $\sigma_{g_{n,i}}$. As in this work we consider a transparent OLS propagation, where each EDFA

978-3-903176-33-1

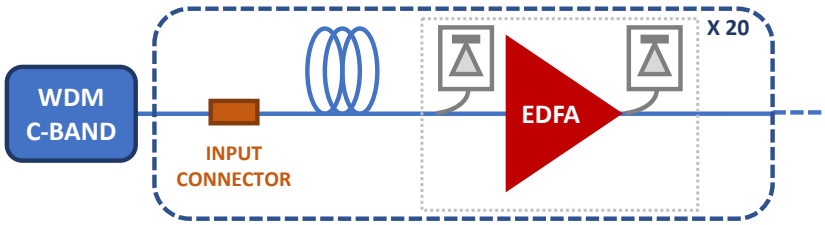

Fig. 1. Layout of the periodic OLS: each span is composed of an input connector, a fiber, an EDFA with input and output monitor photo-diodes.

entirely recover the total fiber loss, A, the expression of the GSNR at the OLS output, for a fixed channel under test (CUT) can be derived from Eq. 1 with a few steps of algebra:

$$\mathrm{GSNR}_{\mathrm{CUT}} = \left\{ \frac{h f_{\mathrm{CUT}} \, \mathrm{NF} \, B_r}{A} \sum_{n=1}^{N_S} \left(l_n P_{ch,n-1}^{\mathrm{CUT}} \right)^{-1} + \sum_{n=1}^{N_S} \left(\sum_{i=1}^{N_{ch}} \left(l_n P_{ch,n-1}^{i} \right)^2 \eta_{i,\mathrm{CUT}} \right) \right\}^{-1} \quad (2)$$

where h is the Planck constant, f_{CUT} is the CUT frequency, $P_{ch,n}^{i}$ is the channel signal power of the i-channel at the n-span, $\eta_{i,j}$ is the power independent matrix characterizing the NLI generation [7] for each couple of channels i, j composing the spectrum, N_S is the number of fiber spans and N_{ch} is the number of spectrum channels. As the considered random variables are independent, it is possible to approximate the standard deviation of the GSNR at the output of the OLS for the CUT by means of the uncertainty propagation expression as follows:

$$\sigma^2_{\mathrm{GSNR}_{\mathrm{CUT}}} \approx \sum_{n=1}^{N_S} \left(\frac{\partial \mathrm{GSNR}_{\mathrm{CUT}}}{\partial l_n} \right)^2 \sigma^2_{l_n} + \sum_{n=1}^{N_S} \sum_{i=1}^{N_{ch}} \left(\frac{\partial \mathrm{GSNR}_{\mathrm{CUT}}}{\partial g_{n,i}} \right)^2 \sigma^2_{g_{n,i}} \quad (3)$$

where $\partial \mathrm{GSNR}_{\mathrm{CUT}} / \partial l_n$ and $\partial \mathrm{GSNR}_{\mathrm{CUT}} / \partial g_{n,i}$ are, respectively, the partial derivatives of the $\mathrm{GSNR}_{\mathrm{CUT}}$ with respect to the input connector loss at the n-span and the gain ripple of the i-channel of the spectrum at the n-span.

III. Monte Carlo Analysis and Results

In order to have an accuracy estimation, the model has been validated by a Monte Carlo analysis framework maintaining the same OLS configurations. In both the analytical and numerical approaches, Gaussian PDFs are assumed for all the random variables. In particular, for each input connector loss we assume a Gaussian distribution of average 0.75 dB and standard deviation 0.28 dB, as shown in Fig. 2. Regarding the EDFA gain ripple profile, we generate a Gaussian PDF for each channel frequency with a distinct average and standard deviation according to the estimations that we obtain from a large experimental data-set of EDFA gain characterizations. In particular, for each channel frequency, the average of the gain ripple ranges within -0.25 dB and 0.3 dB and the standard deviation goes from 0.1 dB to 0.18 dB. The normalized gain ripple profile PDFs vs. frequency are synthetically reported through an heat-map in Fig. 3. The investigated CUT is the central channel of the considered C-band spectrum placed at 193.7 THz.

Each Monte Carlo run generates an OLS in which for each span a connector loss and a complete gain ripple profile are extracted according to the relative PDF of each random variable. We perform the Monte Carlo analysis introducing a flat input power level that sweeps from -6 dBm to 2 dBm per channel for a total number of 13 power levels in order to evaluate the $\mathrm{GSNR}_{\mathrm{CUT}}$ in all the possible working points: linear regime, LOGO [8] and nonlinear regime. In order to achieve stability and convergence, 10^5 Monte Carlo runs are

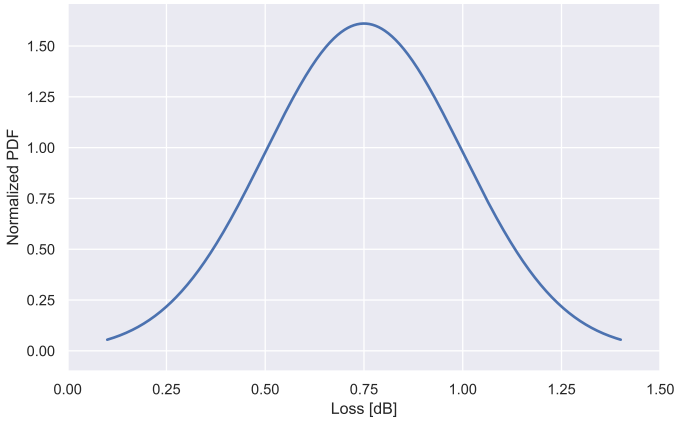

Fig. 2. Input connector loss PDF.

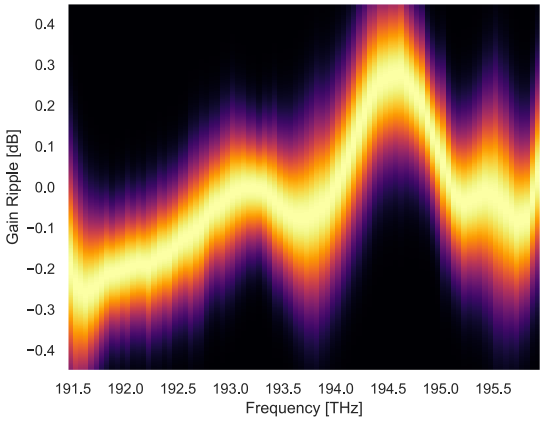

Fig. 3. Heat-map of the normalized gain ripple profile PDF vs. frequency.

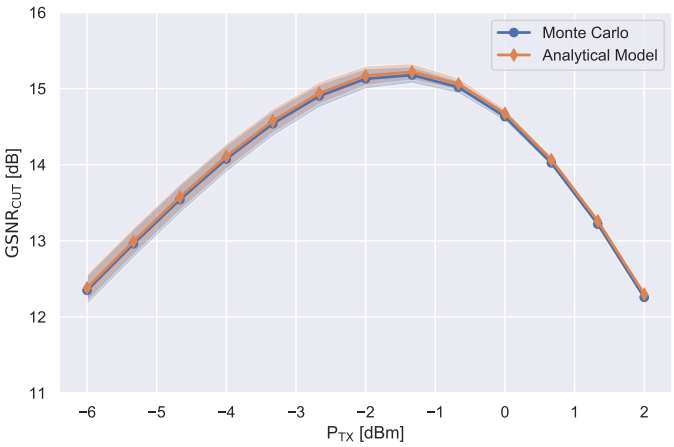

Fig. 4. Average $\mathrm{GSNR}_{\mathrm{CUT}}$ vs. input power level.

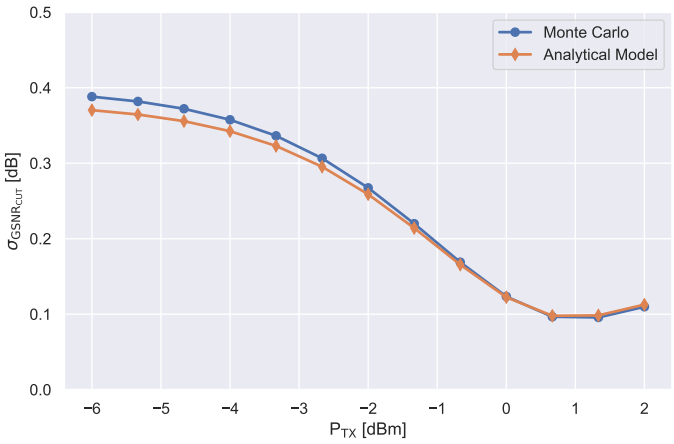

Fig. 5. GSNR standard deviation, $\sigma_{\mathrm{GSNR}_{\mathrm{CUT}}}$, vs. input power level.

performed for each input power level for a total of $1.3 \cdot 10^6$ emulations. On the other hand, we estimate the average $\mathrm{GSNR}_{\mathrm{CUT}}$ and standard deviation $\sigma_{\mathrm{GSNR}_{\mathrm{CUT}}}$ for the complete power sweep through the derived analytical model introducing the corresponding values of average and standard deviation for each random variable.

Results of both Monte Carlo analysis and analytical model are shown in Figs. 4 and 5. The average and standard deviation curves are in complete agreement and this demonstrates the consistency between the two approaches. The proposed analytical model approximates with a significant accuracy the GSNR standard deviation if the input random variables are independent and have symmetrical PDFs. In future works, this approach can be further generalized including asymmetrical distributions.

Observing GSNR average and standard deviation trends, it is possible to draw two key conclusions in operating point selection. Firstly, the optimal launch power level of the scenario under investigation is -1.3 dBm. At this working point, the standard deviation of the GSNR is roughly 0.2 dB; a reduction of the GSNR fluctuations of a factor 2 with respect to the linear regime, where the GSNR standard deviation is approximately 0.4 dB. This reduction implies that the system is more stable with respect to physical layer uncertainties. As a consequence, the selection of the optimal working point mitigates the effects due to the lack of knowledge of the physical layer. Secondly, it can be observed that the GSNR standard deviation minimum is does not correspond to the maximum GSNR. Nevertheless, the launch power with the minimum GSNR standard deviation is beyond the optimal launch power, in a working point dominated by the NLI that induces an unwanted high penalty. Therefore, the best solution for operators is to transmit through the OLS with the optimal launch power level in order to get the maximum capacity and, concurrently, reduce the GSNR fluctuations due to physical layer uncertainties.

IV. Conclusions

We derive a simple analytical model based on uncertainty propagation to estimate the GSNR error due to connector and ILA impairments at the output of a periodic OLS. This methodology has been validated through the comparison with a consistent Monte Carlo analysis, showing a good agreement between the two approaches. As a consequence, this analysis allows to face up the issue related to system margins in lightpath deployment, weighting up the impact of physical layer uncertainties on the quality of transmission.

In future works, we aim to extend the model including any kind of PDF, even asymmetrical ones. We also want to further generalize the formulation taking into account the inter-channel stimulated Raman scattering.

References

[1] G. Forecast, "Cisco visual networking index: global mobile data traffic forecast update, 2017–2022," *Update*, vol. 2017, p. 2022, 2019.

[2] Y. Pointurier, "Design of low-margin optical networks," *Journal of Optical Communications and Networking*, vol. 9, no. 1, pp. A9–A17, 2017.

[3] M. Filer, M. Cantono, A. Ferrari, G. Grammel, G. Galimberti, and V. Curri, "Multi-vendor experimental validation of an open source qot estimator for optical networks," *Journal of Lightwave Technology*, vol. 36, no. 15, pp. 3073–3082, 2018.

[4] V. Curri, "Software-defined wdm optical transport in disaggregated open optical networks," in *2020 22nd International Conference on Transparent Optical Networks (ICTON)*. IEEE, 2020, pp. 1–4.

[5] V. Curri, A. Carena, A. Arduino, G. Bosco, P. Poggiolini, A. Nespola, and F. Forghieri, "Design strategies and merit of system parameters for uniform uncompensated links supporting nyquist-wdm transmission," *Journal of Lightwave Technology*, vol. 33, no. 18, pp. 3921–3932, 2015.

[6] A. Ferrari, G. Borraccini, and V. Curri, "Observing the generalized snr statistics induced by gain/loss uncertainties," in *45th European Conference on Optical Communication (ECOC 2019)*. IET, 2019, pp. 1–4.

[7] P. Poggiolini, G. Bosco, A. Carena, V. Curri, Y. Jiang, and F. Forghieri, "The gn-model of fiber non-linear propagation and its applications," *Journal of lightwave technology*, vol. 32, no. 4, pp. 694–721, 2013.

[8] P. Poggiolini, G. Bosco, A. Carena, R. Cigliutti, V. Curri, F. Forghieri, R. Pastorelli, and S. Piciaccia, "The logon strategy for low-complexity control plane implementation in new-generation flexible networks," in *2013 Optical Fiber Communication Conference and Exposition and the National Fiber Optic Engineers Conference (OFC/NFOEC)*. IEEE, 2013, pp. 1–3.